Defence Research and Development Canada
Recherche et développement pour la défense Canada

DEFENCE R&D DÉFENSE

Auroral clutter observations with a three-dimensional over-the-horizon radar

Ryan J. Riddolls
Defence R&D Canada – Ottawa

Defence R&D Canada – Ottawa

Technical Memorandum
DRDC Ottawa TM 2013-137
November 2013

Canada

Auroral clutter observations with a three-dimensional over-the-horizon radar

Ryan J. Riddolls
Defence R&D Canada – Ottawa

Defence R&D Canada – Ottawa
Technical Memorandum
DRDC Ottawa TM 2013-137
November 2013

Principal Author

Original signed by R. J. Riddolls

R. J. Riddolls

Approved by

Original signed by A. Damini

A. Damini
Acting Head/Radar Systems Section

Approved for release by

Original signed by C. McMillan

C. McMillan
Head/Document Review Panel

© Her Majesty the Queen in Right of Canada as represented by the Minister of National Defence, 2013

© Sa Majesté la Reine (en droit du Canada), telle que représentée par le ministre de la Défense nationale, 2013

Abstract

An Over-the-Horizon Radar (OTHR) has been deployed near Ottawa, Canada. Auroral echoes and ground echoes were analyzed in range, azimuth, elevation, and Doppler. It is shown that the auroral echoes and the ground echoes can be separated in elevation angle.

Résumé

Un radar haute fréquence transhorizon à été déployé près d'Ottawa, Canada. Echos aurorales et échos de sol ont été analysées dans la gamme, l'azimut, l'élévation et Doppler. Il est démontré que les échos aurorales et les échos de sol peuvent être séparés dans l'angle d'élévation.

This page intentionally left blank.

Executive summary

Auroral clutter observations with a three-dimensional over-the-horizon radar

Ryan J. Riddolls; DRDC Ottawa TM 2013-137; Defence R&D Canada – Ottawa; November 2013.

Background:

An Over-the-Horizon Radar (OTHR) has been deployed near Ottawa, Canada. The radar is aimed northward and collects auroral echoes through line-of-sight propagation and ground echoes from beyond the horizon through ionospheric reflection. Previous experiments have demonstrated the suppression of the auroral echo component by forming angular nulls in the transmit and/or receive antenna array beam patterns. The results had been demonstrated exclusively in the Doppler domain, in other words, showing a suppression of various frequency components in the backscatter echo. To date the OTHR project has made no serious attempt to resolve the echoes in spatial dimensions, such as range, azimuth, and elevation, in order to visualize the clutter spatial distribution.

Results:

Auroral echoes have been resolved in the three spatial dimensions of range, azimuth, and elevation, as well as in the temporal dimension of Doppler. The data is interpreted in terms of the theoretical predictions for the clutter distribution. Discussion is provided regarding the feasibility of separating the auroral echoes from the illuminated beyond-the-horizon ground patch echoes. Recommendations are made concerning clutter suppression strategies and future work.

Significance:

The illuminated ground scene, which includes the land and its associated airspace, is of interest for various applications. Auroral clutter, if not properly resolved and filtered out, can mask scatterers of interest within the ground scene. It is shown that three-dimensional spatial resolving capability is useful for separating the ground and auroral echo components.

Future Work:

Three technical deficiencies should be immediately addressed. First, the receive array needs to be expanded to a larger aperture to provide angular resolution comparable to the radar range resolution. A larger receive array will support beamforming in

addition to directional finding, allowing one to resolve range-Doppler coincident objects in azimuth and elevation. Second, the transmit portion of the radar needs to rebuilt to support frequency agile, 100-percent duty cycle operation. Third, a method of spectrum management needs to be implemented, which normally comprises spectrum monitoring and backscattering sounding functionality.

Sommaire

Auroral clutter observations with a three-dimensional over-the-horizon radar

Ryan J. Riddolls; DRDC Ottawa TM 2013-137; Defence R&D Canada – Ottawa; novembre 2013.

Contexte

Nous avons déployé un radar transhorizon près d'Ottawa. Il est dirigé vers le Nord et capte le fouillis auroral par propagation en ligne de vue et des échos de sol d'au-delà l'horizon par réflexion ionosphérique. Des expériences passées ont permis de montrer l'élimination du composant d'écho auroral par la formation de valeurs angulaires nulles dans les diagrammes de faisceaux d'antennes réseau réceptrice ou émettrice (ou les deux). Cependant, ces expériences ne traitaient que du domaine Doppler; en d'autres termes, les résultats montrent l'élimination de divers composants de fréquences dans l'écho de rétrodiffusion. À ce jour, aucune tentative sérieuse de résoudre des échos dans les domaines spatiaux (portée, azimut, site, etc.) n'a été faite dans le cadre du projet de radar transhorizon en vue de visualiser la distribution spatiale du fouillis.

Résultats

Nous avons traité des échos auroraux dans les trois dimensions spatiales : portée, azimut et site, ainsi que dans la dimension temporelle de Doppler. Dans le présent rapport, nous interprétons les données sous forme de prévisions théoriques de la distribution du fouillis. Nous y examinons la faisabilité de séparer les échos auroraux des échos de sol éclairés au-delà de l'horizon. Nous formulons aussi des recommandations sur les stratégies d'élimination du fouillis et proposons des avenues de recherches futures.

Importance

La scène au sol éclairée, qui comprend le sol et son espace aérien connexe, est d'intérêt pour diverses applications. S'il n'est pas traité et filtré correctement, le fouillis auroral peut masquer des diffuseurs d'intérêt de la scène au sol. Dans le présent rapport, nous montrons que la capacité de résolution spatiale 3D est utile pour différencier les composants d'échos auroraux de ceux de sol.

Recherches futures

Il faudrait corriger sans délai trois lacunes techniques. Premièrement, il faut élargir l'ouverture de l'antenne réseau réceptrice afin d'assurer une résolution angulaire comparable à la résolution de portée radar : une antenne réseau plus grande permettra la conformation des faisceaux en plus d'assurer la radiogoniométrie et ainsi de résoudre des objets concurrents dans la portée Doppler en azimut et en élévation. Deuxièmement, il faut reconstruire la portion émettrice du radar pour prendre en charge une exploitation à agilité de fréquence et à facteur d'utilisation de 100 %. Et, enfin, il faut mettre en œuvre une méthode de gestion du spectre, qui comprend normalement la surveillance du spectre et une fonction de sondage de la rétrodiffusion.

This page intentionally left blank.

Table of contents

This page intentionally left blank.

1 Introduction

The work on Over-The-Horizon Radar at Defence R&D Canada (DRDC) had its origins in 2006 when a literature review was conducted to assess the state of the technology from a Canadian perspective [1]. This review motivated theoretical work [2] that was aimed at understanding the potential performance of OTHR technology in Canada. Considerations based on the theoretical Point Spread Function (PSF) and the auroral clutter Radar Cross Section (RCS) suggested that the required clutter cancellation could be as large as 50 dB. It was also shown via the same PSF that adaptive antenna array nulls could be no deeper than about 20 dB for a two-channel adaptive processor. Thus it was hypothesized that if directional nulls could be created on both transmit and receive, that these nulls would combine multiplicatively and increase the suppression of the clutter to a sufficient degree.

An experiment was started in 2009 at a field site in western Ottawa [3]. The field site had been used for HF Surface Wave Radar (HFSWR) experiments from 2004 through to 2009. Surplus HF equipment was available following the completion of the HFSWR experiments. There were challenges in installing electrical ground planes and tall radio masts at the field site, so it was decided to employ a Beverage antenna concept for both the OTHR transmit and receive antenna arrays. This type of antenna consisted a long (multi-wavelength) wire suspended horizontally about 6 m from the ground. By 2010, auroral echoes were obtained using two such antennas on each of transmit and receive [4]. The transmit antennas used distinguishable waveforms, and the receive antennas were independently sampled. The radar was thus a Multiple-Input Multiple-Output (MIMO) system that could produce adaptive nulling on both transmit and receive. It was found that each of the transmit and receive arrays would produce 15-20 dB of nulling of the auroral clutter echoes using a minimum-variance distortionless response (MVDR) beamformer.

After the completion of the above experiment, the apparatus was reworked such that the two-element arrays on transmit and receive were replaced with four-element Beverage antenna arrays on transmit and receive, each arranged in a two-dimensional 2-by-2 pattern [5]. The intent of the experiment was to show that not only do the beam patterns combine on transmit and receive, but that they also combine multiplicatively in the elevation and azimuth directions. The four elements on the transmit side of the radar needed to be fed with distinguishable waveforms to allow non-causal beamforming. To date, however, there has not been sufficient work carried out on the matter of designing waveform sets to run the transmit side of the radar in its intended manner. Thus attention has been focused on the receive side of the radar, with the understanding that adaptive array performance shown for the receive side would also apply to the transmit side since both the transmit and receive arrays have identical antennas and layouts.

The investigation being carried out with the 2-by-2 arrays is aimed at determining whether joint azimuth-elevation beamforming provides enough advantages over azimuth-only or elevation-only beamforming to justify the additional expense of a planar array. Initial work carried out in 2011 [5] looked at receive-only processing of signals of opportunity. An experiment was conducted where a shortwave broadcast signal of opportunity was recorded and subsequently processed in an attempt to null it out in both elevation and azimuth. The total cancellation observed was on the order of 50 decibels, with the elevation and azimuth contributions multiplying as expected. Given that the signal was from a single direction, as opposed to a continuum of directions in the case of auroral clutter, the experiment results were likely optimistic and not representative of the obtainable auroral clutter cancellation. It was decided to repeat the experiment against actual auroral clutter.

Work continued into 2013 to sample the desired auroral ehoes with a two-dimensional array. There was also work on obtaining pulse compression, which required a significant upgrade to the radar hardware in order to produce the required waveforms and processing. By September 2013, auroral clutter echoes were being received by a calibrated two-dimensional receive array, with pulse compression being applied. A single antenna in the transmit array was being used to provide the illumination. This work will be described in this memorandum. In particular, auroral and ground clutter modes are resolved in range, Doppler, azimuth, and elevation in an attempt to provide a clear picture about the requirements for clutter cancellation in an auroral OTHR system.

The remainder of this work is organized into three chapters. Chapter 2 reviews the theoretical basis that will be used to interpret the auroral clutter echoes. Chapter 3 describes the experiment apparatus and provides a presentation of the data. Chapter 4 provides some discussion and suggestions for future work.

2 Theory

In this section we outline some theoretical ideas that will help in interpreting the data to be presented in Section 3. The separability of ionospheric modes lies in their coherency (i.e. phase stability). Two major factors conspire to limit signal coherency. First, the spatial and temporal distribution of clutter-producing scatterers in the auroral plasma determines the angular and Doppler spreads of the clutter. In other words, this distribution determines the shape of the mainlobe of the clutter echo when the echo is resolved by the radar. Second, the propagation to and from the clutter-producing scatterers occurs in an inhomogeneous plasma medium, which produces phase and amplitude scintillations of the radar signal, resulting in a point spread function (PSF). This PSF may have a narrow mainlobe, but the turbulent nature of the plasma medium results in the PSF having significant sidelobes. When interpreting the radar data, we must recall that we are looking at the convolution of the scatterers with the PSF. Thus the impact of the PSF will be most obvious in the clutter sidelobes. If one applies a bandstop spatial filter to remove the clutter mainlobe, the power in the sidelobes will be passed through the filter and will appear as residual clutter. Thus, a careful consideration of the PSF is required in assessing the overall performance of the auroral clutter cancellation scheme. The PSF will be assessed in the second subsection below.

2.1 Clutter distribution

We will consider the scenario of a north-pointed HF radar. Clutter is produced by Bragg scatter from plasma irregularities located in the region of the auroral oval. We thus assume that the clutter-producing scatterers occupy a finite azimuth sector of the radar's field of view. Furthermore, we assume that the scatterers occupy a finite elevation extent due to the localization in height of the ionosphere. Finally, the scatterers are expected to be localized in range if the radar is set up south of the auroral oval. The experimental data presented in Chapter 3 will elucidate the shape of these distributions. For our immediate purposes, we will consider a visualization of the azimuth and elevation sectors as shown in Figure 1. In the figure, the clutter-producing scatterers are considered to originate from within the cuboid region denoted by heavy lines, with the radar located at the origin of coordiates. Radial lines from the radar define the azimuthal and elevation extents of the cuboid volume, whereas the faces at constant range define the clutter range extent.

It is desireable that the radar be instrumented to be able to resolve the cuboid clutter volume from objects outside of the cuboid, but within the radar field of view. This is fairly straightforward in the range dimension, where pulse compression can be used to generate narrow range bins while maintaining good average power. Radars with range resolving capabilities are denoted as one-dimensional radars. Two-dimensional

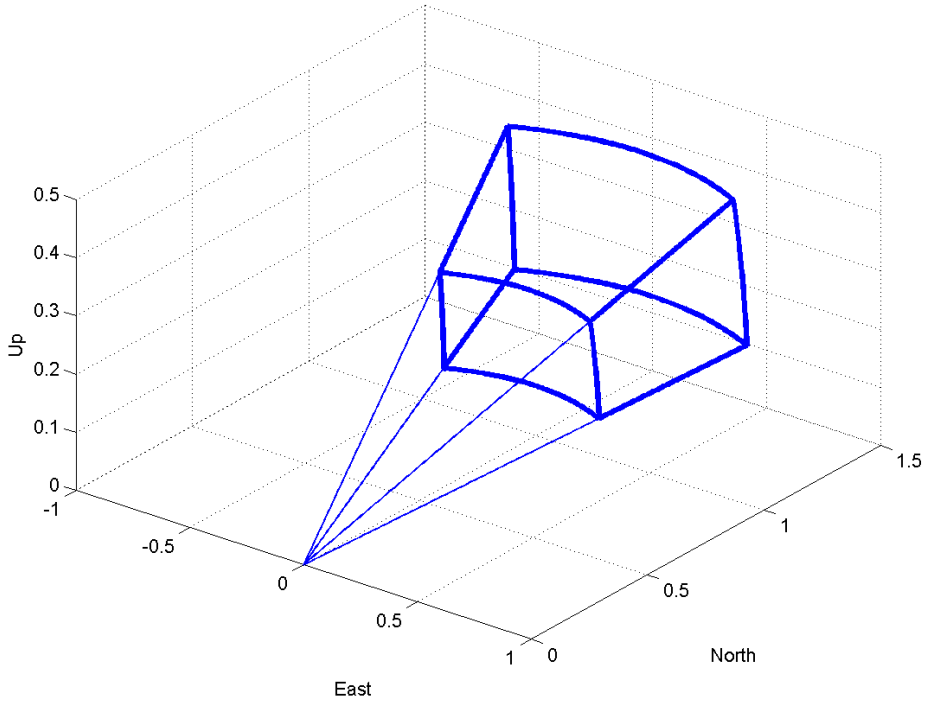

Figure 1: *Visualization of sector occupied by clutter-producing scatterers.*

radars employ both range and azimuth resolution, such that objects could be resolved from clutter even if co-located in range, as long as they are separated in the azimuth extent. Three-dimensional radars add elevation resolving capability, which would allow objects to be resolved from the clutter even if those objects are co-located with the clutter in both range and azimuth.

At this point, we will not make assumptions with regard to the motion of the plasma within the volume occupied by the scatterers. Generally speaking, the action of the solar wind passing the earth drives the auroral ionosphere in a two-cell convection pattern in the horizontal plane, such that the radar observes a clockwise-rotating cell in the evening and a counterclockwise-rotating cell in the morning, with transitions occurring at noon and midnight [6]. Movement of the plasma would cause the clutter to become spread in Doppler. The disadvantage of this occurrence is that the clutter occupies a larger portion of the range-Doppler ambiguity plane, potentially obscuring useful detection cells. The advantage of this occurrence is that it tends to confine the clutter in angle within a particular Doppler cell, a phenomenon sometimes referred to as Doppler beam sharpening. This confinement in angle makes it easier to cancel the clutter through the application of directional nulling in azimuth.

2.2 Scintillation

Signal propagation in inhomogeneous media suffers from the effect of refractive index fluctuations, leading to a randomization (or scintillation) of the signal amplitude and phase. We focus on the phase randomization in this paper as this effect is the dominant influence on the temporal coherence (Doppler spread) and spatial coherence (angle-of-arrival spread) of the radar signal [7, 8].

The phase of a signal at a given point in time is equal to the integration of its spatial rate of change over the ray path:

$$\phi = \int_S k(\mathbf{r})\, ds, \tag{1}$$

where $k(\mathbf{r})$ is the radar signal wavenumber, ds is an element of arc length, S represents the ray path, and $\mathbf{r}$ is a location on S. For simplicity, we take S to be a straight line. A more complicated trajectory, such as a parabolic trajectory in a linear plasma density profile, could also be considered, but it has been shown [2] that this consideration does not change the shape of the resulting phase spectrum. For convenience, we will take the propagation to be in the x direction, which is approximately north and horizontal, for the case of propagation at low elevation angles near radar boresight. We also choose y to be west and z to be up. Let us consider a first-order Taylor series perturbation of $k(\mathbf{r})$ with respect to plasma density n, such that we can write the phase perturbation as

$$\phi_1 = \int n_1(x) \frac{\partial k}{\partial n}\, dx, \tag{2}$$

where n_1 is the plasma density perturbation. For simplicity, we consider an unmagnetized plasma, which has a dispersion relation given by [9]

$$\omega^2 = c^2 k^2 + \frac{e^2 n}{\epsilon_0 m_e}, \tag{3}$$

where ω is the carrier frequency, c is the speed of light, e is the charge on an electron, ϵ_0 is the permittivity of free space, and m_e is the mass of an electron. Using the dispersion relation to compute $\partial k/\partial n$, we arrive at

$$\phi_1 = -r_e \lambda \int n_1(x)\, dx, \tag{4}$$

where $r_e = e^2/(4\pi\epsilon_0 m_e c^2) = 2.8 \times 10^{-15}$ m is the classical electron radius, and λ is the radar wavelength in the plasma. The spatial autocorrelation of ϕ_1 in the horizontal plane is given by

$$R_{\phi_1}(X, Y) = (r_e \lambda)^2 \iint R_{n_1}(X + x - x', Y)\, dx\, dx', \tag{5}$$

where R_{n_1} is the spatial autocorrelation of n_1 in the horizontal plane. After Fourier transforms we have

$$S_{\phi_1}(\kappa_x, \kappa_y) = (r_e\lambda)^2 S_{n_1}(\kappa_x, \kappa_y) \iint e^{i\kappa_x(x-x')}\, dx\, dx' \tag{6}$$

$$= (Lr_e\lambda)^2 \operatorname{sinc}^2(\kappa_x L/2)\, S_{n_1}(\kappa_x, \kappa_y), \tag{7}$$

where L is the distance travelled by the wave packet through the plasma. At high latitudes, we approximate the magnetic field as vertical, so that the plasma organizes itself such that S_{n_1} is rotationally symmetric around a vertical axis. For a two-dimensional turbulent plasma, the Kolmogorov turbulence spectrum has a $\kappa^{-8/3}$ dependence, which we approximate as κ^{-3} [10, 11]:

$$S_{n_1}(\kappa_x, \kappa_y) = \frac{2\pi\kappa_0 \left\langle n_1^2 \right\rangle}{(\kappa_0^2 + \kappa_x^2 + \kappa_y^2)^{3/2}}, \tag{8}$$

where κ_0 is the inverse scale length of the largest turbulent eddies. The spectrum is normalized as follows:

$$\left\langle n_1^2 \right\rangle = \frac{1}{(2\pi)^2} \int_{-\infty}^{\infty}\int_{-\infty}^{\infty} S_{n_1}(\kappa_x, \kappa_y)\, d\kappa_x\, d\kappa_y. \tag{9}$$

If we insert (8) in (7) and take inverse Fourier transforms, we have

$$R_{\phi_1}(X, Y) = \frac{\kappa_0 (Lr_e\lambda)^2 \left\langle n_1^2 \right\rangle}{2\pi} \int_{-\infty}^{\infty}\int_{-\infty}^{\infty} \frac{\operatorname{sinc}^2(\kappa_x L/2)\, e^{i\kappa_x X + i\kappa_y Y}\, d\kappa_x\, d\kappa_y}{(\kappa_0^2 + \kappa_x^2 + \kappa_y^2)^{3/2}}. \tag{10}$$

We recall the identity

$$\frac{2|u| K_1(a|u|)}{a} = \int_{-\infty}^{\infty} \frac{e^{iux}\, dx}{(a^2 + x^2)^{3/2}}, \tag{11}$$

where K_1 is the modified Bessel function of the second kind. By using (11) we find

$$R_{\phi_1}(X, Y) = \frac{\kappa_0 (Lr_e\lambda)^2 \left\langle n_1^2 \right\rangle}{\pi} \int_{-\infty}^{\infty} \operatorname{sinc}^2(\kappa_x L/2) \frac{|Y| K_1\left[(\kappa_0^2 + \kappa_x^2)^{1/2} |Y|\right]}{(\kappa_0^2 + \kappa_x^2)^{1/2}} e^{i\kappa_x X}\, d\kappa_x. \tag{12}$$

Under the condition $5 \times 10^5\,\mathrm{m} \approx L \gg \kappa_0^{-1} \approx 10^4\,\mathrm{m}$, the factor $\operatorname{sinc}^2(\kappa_x L/2)$ acts as a Dirac delta function with respect to factors of $(\kappa_0^2 + \kappa_x^2)^{1/2}$. Hence

$$R_{\phi_1}(X, Y) = 2(Lr_e\lambda)^2 \left\langle n_1^2 \right\rangle |Y| K_1(\kappa_0|Y|) \frac{1}{2\pi} \int_{-\infty}^{\infty} \operatorname{sinc}^2(\kappa_x L/2) e^{i\kappa_x X}\, d\kappa_x. \tag{13}$$

We note the Fourier transform relationship

$$\frac{1}{2\pi} \int_{-\infty}^{\infty} \operatorname{sinc}^2(\kappa_x L/2) e^{i\kappa_x X}\, d\kappa_x = \frac{1}{L} \operatorname{tri}(X/L), \tag{14}$$

where tri(x) $= (1 - |x|)\mu(1 - |x|)$ is the triangle function, and $\mu(x)$ is the unit step function. The final form of the correlation function is therefore

$$R_{\phi_1}(X, Y) = 2L(r_e\lambda)^2 \left\langle n_1^2 \right\rangle \text{ tri}\,(X/L)\ |Y| K_1(\kappa_0|Y|). \tag{15}$$

The mean-square value of ϕ_1 is

$$\left\langle \phi_1^2 \right\rangle = R_{\phi_1}(0, 0) = \frac{2L(r_e\lambda)^2 \left\langle n_1^2 \right\rangle}{\kappa_0}. \tag{16}$$

As an example, let us consider $L = 500$ km, $\lambda = 30$ m, and $\langle n_1^2 \rangle = 10^{18}$ m^{-6}, which represents 1-percent density fluctuations of a peak ionosphere density of 10^{11} m^{-3}. This gives us a root-mean-square phase fluctuation $\sqrt{\langle \phi_1^2 \rangle}$ on the order of 10 radians.

Unfortunately, radars do not measure the phase ϕ_1 directly. Rather, they measure a complex signal amplitude $A = e^{i\phi_1}$. The autocorrelation of the complex signal amplitude A can be related to the autocorrelation of the phase ϕ_1 by [12]:

$$R_A(X, Y) = \left\langle e^{-i\phi_1(x,y)} e^{i\phi_1(x+X, y+Y)} \right\rangle = e^{R_{\phi_1}(X,Y) - \left\langle \phi_1^2 \right\rangle}. \tag{17}$$

The complex amplitude autocorrelation function is

$$R_A(X, Y) = e^{-\left\langle \phi_1^2 \right\rangle [1 - \text{tri}(X/L)\kappa_0 |Y| K_1(\kappa_0|Y|)]}. \tag{18}$$

The angular PSF is essentially the Fourier transform of the autocorrelation function. $R_A(X, Y)$ is not a separable function in X and Y, so the two-dimensional Fourier transform

$$S_A(\kappa_x, \kappa_y) = \int_{-\infty}^{\infty} \int_{-\infty}^{\infty} R_A(X, Y) e^{-i\kappa_x X - i\kappa_y Y}\, dX\, dY, \tag{19}$$

is not tractable. However, the marginal spectra are more manageable:

$$S_A(\kappa_x) = \int_{-\infty}^{\infty} R_A(X, 0) e^{-i\kappa_x X}\, dX \tag{20}$$

$$S_A(\kappa_y) = \int_{-\infty}^{\infty} R_A(0, Y) e^{-i\kappa_y Y}\, dY. \tag{21}$$

In the case of $S_A(\kappa_x)$, we approximate $R_A(X, 0)$ as

$$R_A(X, 0) \approx e^{-\left\langle \phi_1^2 \right\rangle |X|/L}, \tag{22}$$

such that the approximation is good where the function is non-negligible. For $\langle \phi^2 \rangle \approx 100$ and $L \approx 500$ km, the correlation length in the endfire direction (along the ground path underneath the ray) is about 5 km. The marginal spectra in the x direction is the well-known Fourier transform:

$$S_A(\kappa_x) = \frac{2\left\langle \phi_1^2 \right\rangle / L}{\left(\left\langle \phi_1^2 \right\rangle / L\right)^2 + \kappa_x^2}. \tag{23}$$

This spectrum has unit area, with two-sided width of $\Delta\kappa_x = 2\left\langle\phi_1^2\right\rangle/L$, and second-order sidelobe rolloff. At 10 MHz, the radar radial wavenumber is $k = 0.21$ m^{-1}, so for a beam elevation of $\theta = 10$ degrees, the best realizable elevation resolution is $\Delta\theta = \Delta\kappa_x/(k\sin\theta) \approx 0.6$ degrees. Thus the mainlobe spread is quite small, but the sidelobe rolloff is rather slow. For example, at a separation of 10 degrees from the mainlobe (30 times the one-sided mainlobe width), the sidelobes are at best 30 dB down.

In the case of $S_A(\kappa_y)$, the transform is not tractable, but one can estimate its width and sidelobe rolloff rate. Using the small-argument expansion of $zK_1(z)$ [13]:

$$zK_1(z) \approx 1 + (z^2/2)\log(z/2), \tag{24}$$

one can approximate $R_A(0, Y)$ as

$$R_A(0, Y) \approx e^{\left\langle\phi_1^2\right\rangle(\kappa_0|Y|)^2\log(\kappa_0|Y|/2)/2}, \tag{25}$$

such that the approximation is good where the function is non-negligible. Disregarding the slowly-varying (and near-unity) logarithm factor, we estimate the one-sided width of the above function as approximately $(\kappa_0\sqrt{\langle\phi_1^2\rangle})^{-1}$, and thus the one-sided width of its Fourier transform is approximately $\kappa_0\sqrt{\langle\phi_1^2\rangle}$. Furthermore, by taking derivatives of the above expression, one can show that only the first two derivatives are continuous at the origin, which indicates a fourth-order sidelobe rolloff. The Fourier transform is thus approximately

$$S_A(\kappa_y) = \frac{2\kappa_0^3\left\langle\phi_1^2\right\rangle^{3/2}}{(\kappa_0^2\left\langle\phi_1^2\right\rangle + \kappa_y^2)^2}, \tag{26}$$

where the spectrum has been normalized to unit area. The (two-sided) width of the transform should therefore be approximately $\Delta\kappa_y = 2\times10^{-3}$ m^{-1}. At 10 MHz, the radar radial wavenumber is $k = 0.21$ m^{-1}, so the best realizable azimuth resolution is $\Delta\varphi = \Delta\kappa_y/k \approx 0.6$ degree, which is similar to the elevation resolution. However, the sidelobes have fourth-order as opposed to second-order rolloff, meaning that at a separation of 10 degrees, the sidelobes can be as much as 60 dB down. This means that the cancellation of auroral clutter will be easier in azimuth than in elevation.

3 Experiment

This section is organized into two subsections. The first subsection describes the experiment apparatus. The second subsection presents and interprets the data.

3.1 Apparatus

An experimental OTHR is installed at the DRDC campus in Ottawa, Canada. Figure 2 shows the placement of antennas at the site. The OTHR features an array of eight Beverage antenna elements, laid out in a 4-by-2 configuration, with four for transmit, and four for receive. These antennas were selected for the experiment because they do not require ground planes or towers. The antennas are 150 m long and suspended 6 m above the ground. The antennas generate about 1 dBi of gain at 5 MHz in the magnetic north direction, where one expects to receive strong auroral clutter echoes. Each of the four transmit antennas can be excited with independent waveforms at 4 kW peak power and up to 100-percent duty cycle, and each of the four receive antennas is connected to a digital receiver.

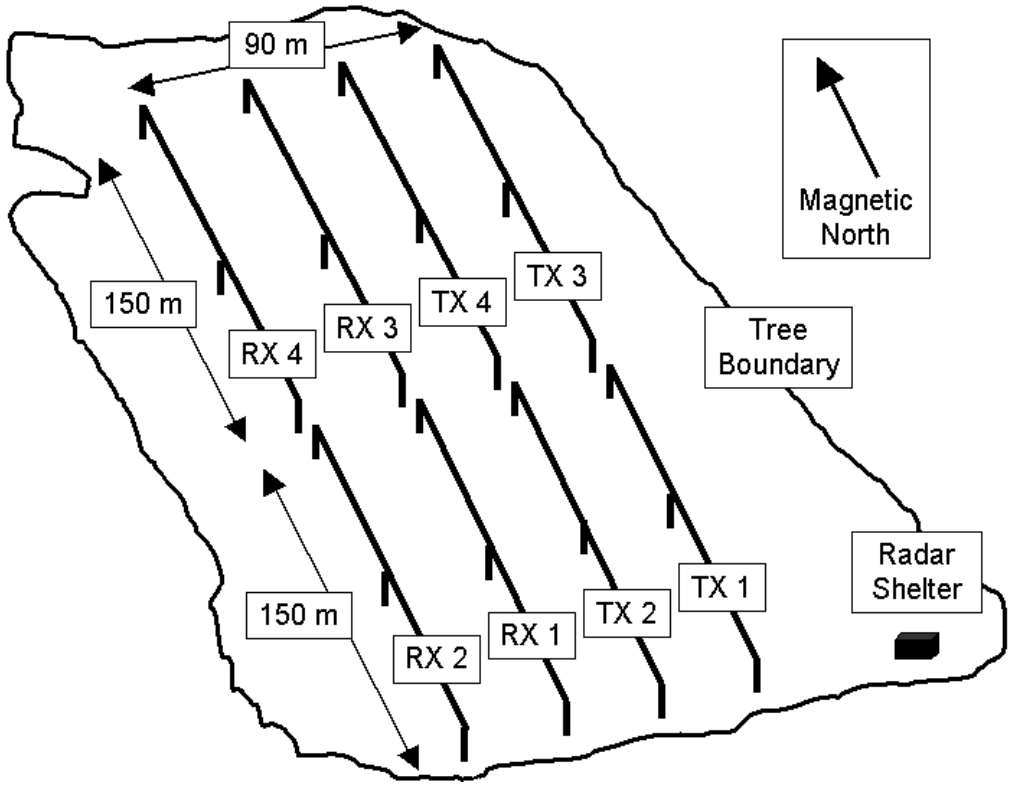

Figure 2: *Site layout. TX1 through TX4 are the transmit antennas and RX1 through RX4 are the receive antennas.*

As stated in the introduction, to date there has not been sufficient work carried out on the matter of designing waveform sets to run the transmit side of the radar in its intended manner. Thus attention has been focused on the receive side of the radar, with the understanding that adaptive array performance shown for the receive side would also apply to the transmit side since both the transmit and receive arrays have identical antennas and layouts. For this work, a single antenna in the transmit array is being used to provide the illumination. Auroral clutter modes are resolved in range, Doppler, azimuth, and elevation in an attempt to provide a clear picture about the requirements for clutter cancellation in an auroral OTHR system.

With regard to the resolution parameters, the system employs a linear chirped waveform with a bandwidth of 3 kHz. When pulse-compressed, this bandwidth provides a range resolution of 50 km. The pulse repetition frequency is 50 Hz, which provides an unambiguous range extent of 3,000 km. To maximize signal-to-noise ratio, the duty cycle is 50 percent. Thus pulse compression is only complete at a single range of 1,500 km, where the echoes of the transmit waveform appear entirely within the receive window. As one moves away from 1,500 km, parts of the echo are blanked out by the transmission, leading to incomplete pulse compression. The resulting range processing is of adequate quality between 750 km and 2,250 km, but starts to degrade noticeably at ranges closer than 750 km and ranges farther than 2,250 km. These problems could be remedied by using a receive array spaced a sufficient distance from the transmit array in order to avoid blanking the receiver during the transmit pulse.

The Doppler processing has a bandwidth of ± 25 Hz, as determined by the radar pulse repetition frequency (PRF) of 50 Hz. The number of pulses in a data set is 1000, or 20 seconds of data, which leads to a Doppler resolution of 0.05 Hz. This number of cells often exceeds the coherence time of the ionosphere, so some smearing in the Doppler domain might be expected.

With regard to angular processing, the antennas are spaced by one-half wavelength in the broadside (azimuth) extent, which provides full ± 90 degrees unambiguous direction finding in the azimuth domain. Because of the length of the Beverage antennas in the endfire direction, the array spacing in that dimension is 2.5 wavelengths, which means that when steered endfire, the unambiguous elevation domain extends from the horizon (0 degrees elevation) to an elevation angle of 53 degrees, which is adequate for elevation-finding of target echoes.

The small 2-by-2 array used on receive provides only coarse angular resolution on the order of a radian. To obtain higher resolution, we estimate the elevation and azimuth angular spectra using a stochastic direction-finding technique [14]. This technique is based on the idea that a power-weighted histogram of the measured spatial phase lags between two antennas is equal to the wavenumber spectrum of the wavefield being measured. This technique generally works if the statistics of the wavefield are

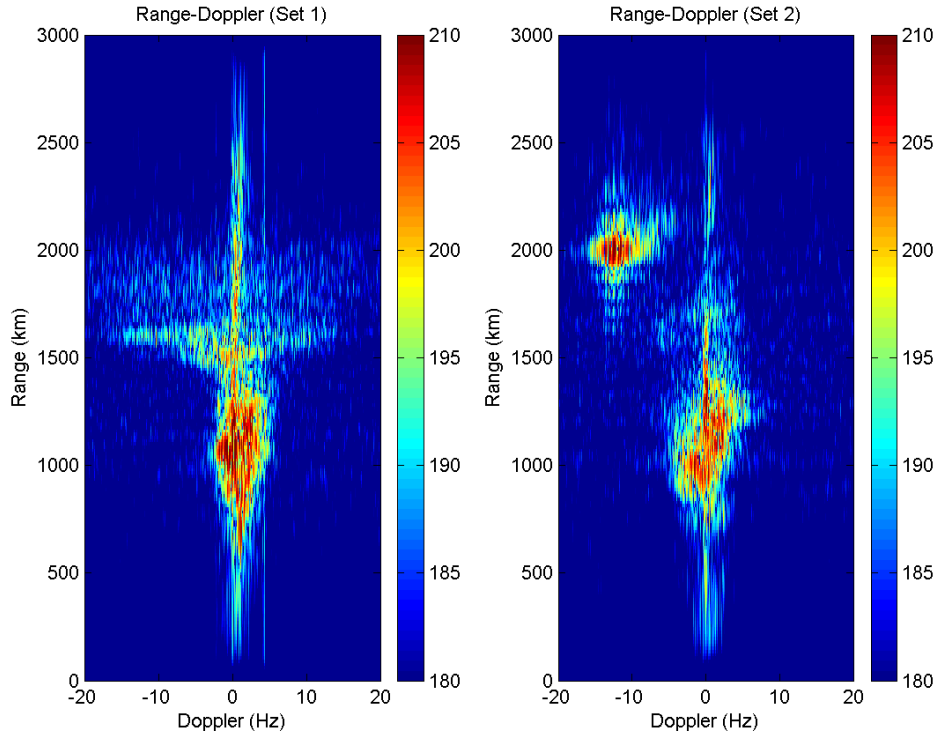

Figure 3: *Range-Doppler maps of Set 1 and Set 2.*

stationary over a distance large compared to the wavelengths of the wavefield. As is the case with most direction-finding techniques, the stochastic direction-finding can improve the apparent resolution compared to beamforming by the squareroot of the signal-to-noise ratio. The nonlinearity of the technique, however, can occasionally result in weak modes disappearing in the presence of nearby strong modes. This effect is somewhat analogous to the so-called capture effect in FM reception, where only the stronger of two signals in the passband of the receiver is demodulated. The effect will be noted when the technique is used to generate plots of radar echoes on range-elevation and range-azimuth axes in the next section.

3.2 Results

Two data sets will be presented in this section. The sets were collected on 13 Sep 2013 at 0637 and 0844 UTC. Figure 3 shows range-Doppler processed data for Set 1 and Set 2. In both sets we see ground clutter at 0 Hz extending through much of the unambiguous range, with Doppler-spreading of the ground clutter evident between about 800 km and 1,300 km in range. In Set 1, auroral clutter is evident between about 1,400 km and 1,900 km in range, and spread over about $\pm$15 Hz in Doppler. In

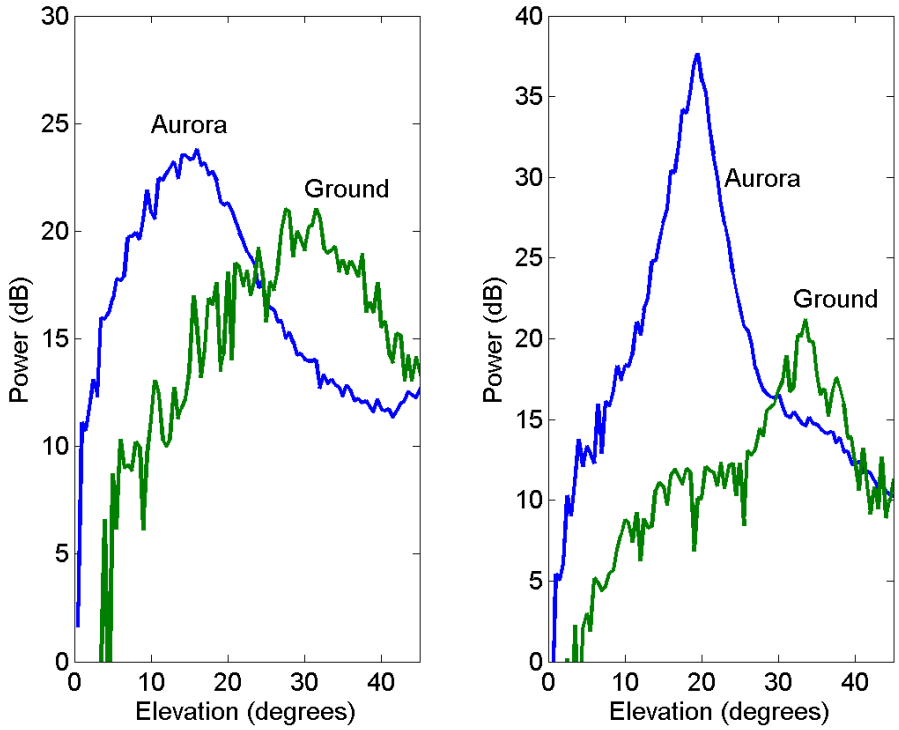

Figure 4: *Elevation distributions of Set 1 and Set 2.*

Set 2, the auroral clutter is located between about 1,800 km and 2,200 km in range, and spread between about -19 Hz and -7 Hz in Doppler. These data sets show that the range-Doppler locations and spreadings of the auroral clutter are variable with time, and a clutter rejection scheme must be flexible to accommodate these variations. Furthermore, the auroral clutter in Set 1 is clearly co-located in range and Doppler with ground clutter, so the ground scene could be masked by the auroral clutter. In Set 2, the auroral clutter is clearly separated from ground clutter in Doppler, although the auroral clutter still occurs at the same range as the ground clutter. In this case, the illuminated ground scene would be masked if elements of the scene produced Doppler shifts in the Doppler extent occupied by the auroral clutter.

Figure 4 shows elevation processed data for Set 1 and Set 2. To create these plots, data were selected from the range-Doppler plots of Figure 3 to represent either ground clutter or auroral clutter. For both data sets, we focused attention on the range interval of 1,500 km to 2,250 km. Within that range interval, the Doppler interval of -0.5 Hz to 0.5 Hz was selected to represent ground clutter and the interval of -20 Hz to -0.5 Hz was selected to represent auroral clutter. Elevation estimates were produced following the method of [14]. For Set 1 in Figure 4 the green trace shows the ground clutter and the blue trace shown the auroral clutter. The distributions

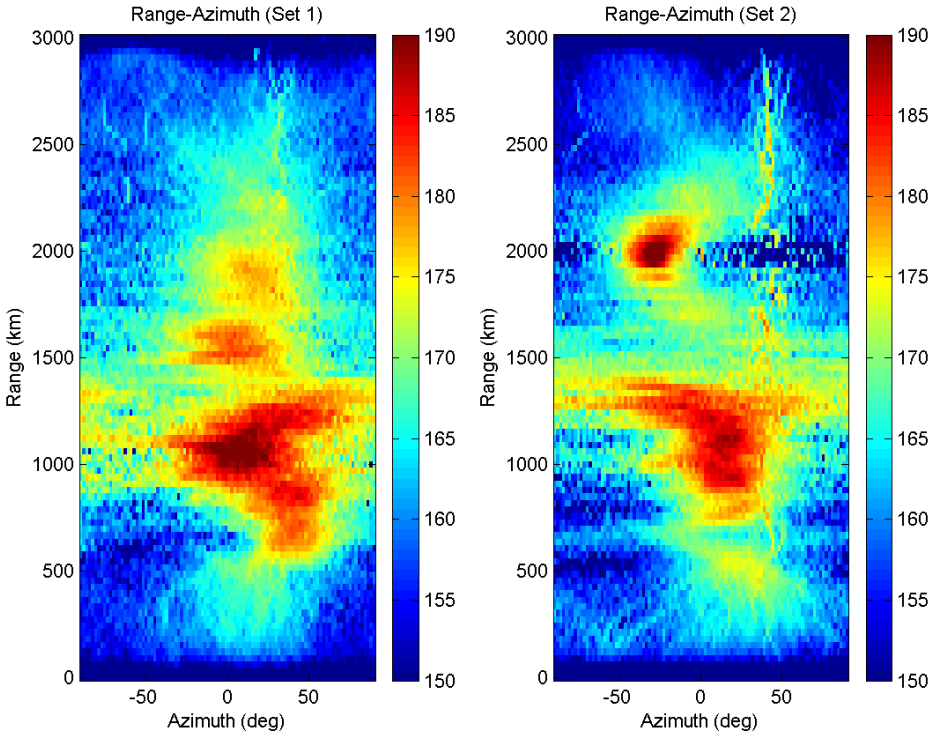

Figure 5: *Range-azimuth maps of Set 1 and Set 2.*

are separated by about 15 degrees. To resolve this separation at frequencies down to 5 MHz, one needs a vertical aperture of about 250 m, which at an elevation of 15 degrees corresponds to a requirement for a ground-based 1-km endfire array.

In Set 2, the separation between the ground and auroral clutter has shrunk to about 10 degrees, but has moved up about 5 degrees in elevation. To obtain a resolution of 10 degrees at frequencies down to 5 MHz, one requires a vertical aperture of about 350 m, which at an elevation of 20 degrees corresponds again to a requirement for a ground-based 1-km endfire array. Also to be noted in these data sets are the slow sidelobe rolloffs in elevation suggested by the PSF from the theory, where we calculated rolloffs no better than 30 dB for a 10-degree separation in elevation from the auroral clutter echo. In the data sets, the rolloff appears to be bounded by the rate of 30 dB for a 10-degree separation, especially in Set 2. Thus one would likely need elevation processing on both transmit and receive if one wanted to separate ground and auroral modes purely in elevation.

Figure 5 shows range-azimuth processed data for Set 1 and Set 2. One must bear in mind that the response in the azimuth direction is somewhat impacted by the azimuthal response of the antennas, which tends to roll off outside ± 30 degrees azimuth.

With this in mind, we turn to Set 1, where we see that the ground echo occupies a fairly large azimuth extent of -40 to about 70 degrees, whereas the auroral clutter modes are more localized in azimuth, with the two auroral modes being localized to -30 to 30 degrees and -10 to 40 degrees, respectively. We found earlier that the PSF is well-localized in azimuth (estimated as up to 60 dB rolloff at 10-degree offset) so the slow rolloffs that are observed in these images are likely due to the clutter distribution in azimuth as opposed to the PSF. This is not surprising, since the bottomside ionosphere has a large horizontal extent relative to the vertical extent, and thus one might expect graceful tapering of the distributions in azimuth. Nevertheless, the auroral clutter is more confined in azimuth than the ground clutter, suggesting an opportunity to resolve the auroral clutter from the ground clutter.

In Set 2, we see an even more localized auroral clutter mode, occupying the azimuth extent -50 to -10 degrees, leaving positive azimuth clear. It should be noted, however, that the blue horizontal bar seen at 2,000-km range is likely an artifact of the azimuth estimation technique [14]. The angle estimates for range bins near 2,000 km are dominated by the auroral clutter returns and thus other phase lags are suppressed. This effect is somewhat analogous to the so-called capture effect in FM reception, where only the stronger of two signals in the passband of the receiver is demodulated. We also note that an interference signal seen at about 40 degrees azimuth is similarly suppressed around 2,000 km.

Although the theory did not explicitly consider plasma motion, there is the possibility that plasma motion could produce an auroral clutter Doppler signature that could be exploited. Thus we examine the auroral clutter in Doppler-azimuth coordinates. In Figure 6 we see Doppler-azimuth processed results for Set 1 and Set 2, including all the data at ranges beyond 1,500 km.

In Set 1, we see the ground clutter as a horizontal band near 0 Hz. An interference signal is seen at about 4 Hz, originating about -50 degrees in azimuth. The auroral clutter has some azimuth and Doppler dependence. At -15 Hz Doppler, the clutter is centered at about -20 degrees azimuth, whereas at 15 Hz Doppler, the clutter is centered at about 20 degrees azimuth. This phenomenon suggests that the clutter includes echoes from a rotating plasma convection pattern. The implication is that Space-Time Adaptive Processing (STAP) may be useful in this context to take advantage of the Doppler-azimuth coupling.

In Set 2, the auroral clutter is significantly localized in Doppler-azimuth, as might be expected by examination of the range-Doppler and range-azimuth maps. There is, however, a tail structure leading from the auroral clutter back to the coordinate origin that could be addressed through STAP. Also evident in this image is the ground clutter at 0 Hz, a narrowband interference signal at 4 Hz, and a broadband interference signal at around 40 degrees azimuth. The broadband interference was

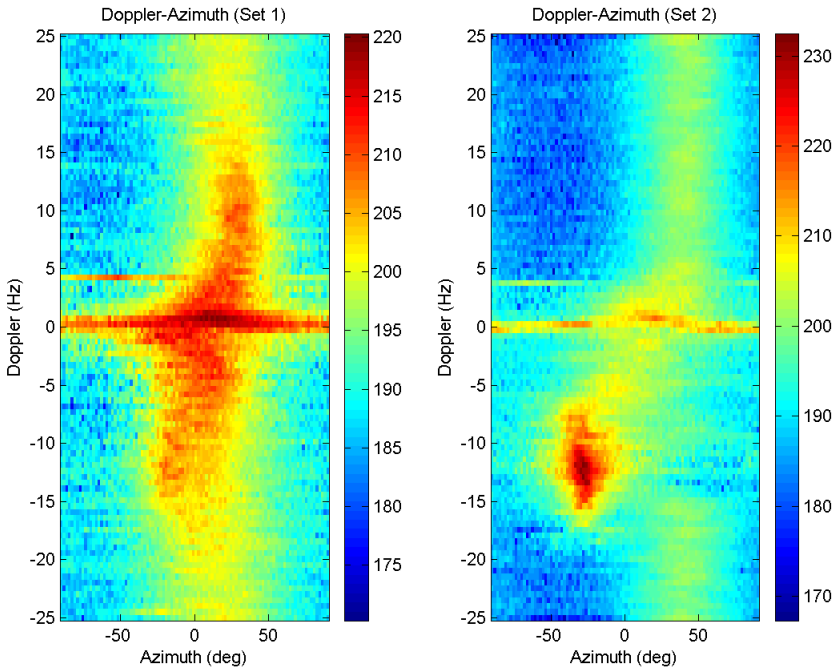

Figure 6: *Doppler-azimuth maps of Set 1 and Set 2.*

also seen in Figure 3. Furthermore, the capture effect is also visible in this figure in the manner in which the broadband source has been suppressed in the Doppler frequency range between -15 and -5 Hz. A more robust spectral estimator could be realized with a large beamforming array, perhaps in a shape of a cross in order to resolve both the azimuth and elevation extents with good resolution.

4 Conclusion

This memorandum has presented data sets showing the resolution of auroral clutter and ground clutter modes in range, Doppler, azimuth, and elevation, which represents a considerable advance in data collection capability compared to previous efforts that could only resolve in Doppler. Features of these data sets have been discussed in regard to the feasibility of different strategies for the separation of auroral echoes from ground echoes. Although the available data set is limited, some preliminary observations can be made, as discussed below.

First, the auroral echoes do not necessarily coincide in range with echoes from the ground scene. In these cases, no angular filtering at all is required to maintain visibility of the ground. It is therefore recommended that frequency selection algorithms for the radar automatically detect whether particular candidate operating frequencies feature a range separation of the auroral and ground clutter components.

Second, if targets are co-located in range, then elevation separation may be feasible, as the auroral echoes were generally observed below 10 to 15 degrees elevation, whereas ground echoes would generally be above this angle. One can contemplate a bandstop spatial filter that would remove the auroral clutter coming from the lowest-elevation regions of the illuminated volume. The limitation of the elevation resolution is the PSF due to propagation through inhomogeneous ionospheric plasma. In particular, propagation through a finite-thickness sheet of plasma irregularities results in a spatial decorrelation of the radar signal in the endfire direction. The decorrelation results in a PSF that decays by about 30 dB at a separation of 10 degrees. This limited clutter confinement suggests a recommendation that elevation filtering should be carried out on both transmit and receive, which would double the clutter suppression on a dB scale.

Third, if targets cannot be resolved in elevation, there is the possibility of resolving in azimuth angle. It was shown that the theoretical azimuth sidelobes of the PSF are around 60 dB down at 10 degrees separation. This confinement suggests the recommendation that antenna arrays be layed out to try to take advantage of azimuthal separation. These could be realized by overlapping radar coverage of areas from different angles. It was also noted that there is often a Doppler-azimuth coupling of the clutter echoes, which would suggest that STAP may be a useful means by which to suppress the auroral clutter component.

The work has also highlighted deficiencies in the technology that should be targeted for future work, as described below.

First, the receive array needs to be expanded to a larger aperture to provide adequate resolution to locate targets. A large (1-km) receive array is being planned for instal-

lation in 2014 at a site about 20 km west of the existing OTHR experiment site. The receive array will support quasi-monostatic experiments with a transmitter at the existing OTHR site. Separating the transmit and receive portions of the radar allows one to use continuous-wave waveforms, which have a number of desirable features.

Second, the transmit portion of the DRDC radar needs to be rebuilt with new antennas and new transmission line. The existing Beverage antennas as implemented have limited bandwidth, limited azimuth illumination, and tend to collapse during snow and ice events in the winter. The existing transmission line is under-sized for the power levels currently being used and has been suffering from water infiltration, leading to arcing. New transmitters may also be required as the existing transmitters have obsolete parts and are under-designed for the application, leading to overheating problems.

Third, a method of spectrum management needs to be developed for the radar. Currently the radar is licensed to operate on a single frequency near 5 MHz. To get continuous illumination of downrange areas, however, one has to continuously adjust the radar carrier frequency to accommodate changes in the electron density of the ionosphere plasma over the course of the day and night. To determine required frequencies, the radar must initially sweep the HF spectrum and determine the group range of ground backscatter (and possibly auroral clutter) versus carrier frequency. Once the range of usable carrier frequencies is identified, the radar must find a channel within that range that is not occupied by existing users of the HF spectrum, and then automatically retune the radar. This whole process of spectrum management needs to be implemented in the radar.

References

[1] Riddolls, R. J. (2006). A Canadian perspective on high-frequency over-the-horizon radar, (DRDC Ottawa TM 2006-285) Defence R&D Canada—Ottawa.

[2] Riddolls, R. J. (2008). Detection of aircraft by high frequency sky wave radar under auroral clutter-limited conditions, (DRDC Ottawa TM 2008-336) Defence R&D Canada—Ottawa.

[3] Riddolls, R. J. (2009). Initial results of HF sky wave radar experiments using MIMO methods to control auroral clutter, (DRDC Ottawa TM 2009-268) Defence R&D Canada—Ottawa.

[4] Riddolls, R. J. (2010). Auroral clutter mitigation in an over-the-horizon radar using joint transmit-receive adaptive beamforming, (DRDC Ottawa TM 2010-265) Defence R&D Canada—Ottawa.

[5] Riddolls, R. J. (2012). Hyperspace aperture concept for auroral clutter control in a Canadian over-the-horizon radar, (DRDC Ottawa TM 2012-159) Defence R&D Canada—Ottawa.

[6] Kelley, M. C. (1989). The Earth's ionosphere. San Diego: Academic Press.

[7] Wheelon, A. D. (2001). Electromagnetic scintillation, Volume 1, geometric optics. New York: Cambridge University Press.

[8] Ravan, M., Riddolls, R. J., Adve, R. S. (2012). Ionospheric and auroral clutter models for HF surface wave and over the horizon radar systems, *Radio Sci.*, 47, doi: 10.1029/2011RS004944.

[9] Budden, K. G. (1985). The propagation of radio waves: the theory of radio waves of low power in the ionosphere and magnetosphere. New York: Cambridge University Press.

[10] Woodman, R. F., Basu, S. (1978). Comparison between in-situ spectral measurements of F-region irregularities and backscatter observations at 3-meter wavelength, *Geophys. Res. Lett.*, 5, 869–872, doi:10.1029/GL005i010p00869.

[11] Vallieres, X., Villain, J. P., Hanuise, C., Andre, R. (2004). Ionospheric propagation effects on spectral widths measured by Superdarn HF radars, *Ann. Geophys.*, 22, 2023–2031.

[12] Reed, I. S. (1962). On a moment theorem for complex Gaussian processes. *IRE Transactions on Information Theory*, 8 (4), 194–195.

[13] Abramowitz, M. and Stegun, I. A. (1964). Handbook of mathematical functions with formulas, graphs, and mathematical tables. New York: Dover.

[14] Beall, J. M., Kim, Y. C., and Powers E. J. (1982). Estimation of wavenumber and frequency spectra using fixed probe pairs. *Journal of Applied Physics*, 53 (6), 3933-3940.

DOCUMENT CONTROL DATA

(Security classification of title, body of abstract and indexing annotation must be entered when document is classified)

1. ORIGINATOR (the name and address of the organization preparing the document. Organizations for whom the document was prepared, e.g. Centre sponsoring a contractor's report, or tasking agency, are entered in section 8.)

   Defence R&D Canada – Ottawa
   3701 Carling Avenue, Ottawa, Ontario, Canada K1A 0Z4

2. SECURITY CLASSIFICATION (overall security classification of the document including special warning terms if applicable).

   UNCLASSIFIED
   (NON-CONTROLLED GOODS)
   DMC A
   REVIEW: GCEC APRIL 2011

3. TITLE (the complete document title as indicated on the title page. Its classification should be indicated by the appropriate abbreviation (S,C,R or U) in parentheses after the title).

   Auroral clutter observations with a three-dimensional over-the-horizon radar

4. AUTHORS (last name, first name, middle initial)

   Riddolls, Ryan J.

5. DATE OF PUBLICATION (month and year of publication of document)	6a. NO. OF PAGES (total containing information. Include Annexes, Appendices, etc).	6b. NO. OF REFS (total cited in document)
November 2013	32	14

7. DESCRIPTIVE NOTES (the category of the document, e.g. technical report, technical note or memorandum. If appropriate, enter the type of report, e.g. interim, progress, summary, annual or final. Give the inclusive dates when a specific reporting period is covered).

   Technical Memorandum

8. SPONSORING ACTIVITY (the name of the department project office or laboratory sponsoring the research and development. Include address).

   Defence R&D Canada – Ottawa
   3701 Carling Avenue, Ottawa, Ontario, Canada K1A 0Z4

9a. PROJECT NO. (the applicable research and development project number under which the document was written. Specify whether project).	9b. GRANT OR CONTRACT NO. (if appropriate, the applicable number under which the document was written).
03mz08	

10a. ORIGINATOR'S DOCUMENT NUMBER (the official document number by which the document is identified by the originating activity. This number must be unique.)	10b. OTHER DOCUMENT NOs. (Any other numbers which may be assigned this document either by the originator or by the sponsor.)
DRDC Ottawa TM 2013-137	

11. DOCUMENT AVAILABILITY (any limitations on further dissemination of the document, other than those imposed by security classification)

    (X) Unlimited distribution
    ( ) Defence departments and defence contractors; further distribution only as approved
    ( ) Defence departments and Canadian defence contractors; further distribution only as approved
    ( ) Government departments and agencies; further distribution only as approved
    ( ) Defence departments; further distribution only as approved
    ( ) Other (please specify):

12. DOCUMENT ANNOUNCEMENT (any limitation to the bibliographic announcement of this document. This will normally correspond to the Document Availability (11). However, where further distribution beyond the audience specified in (11) is possible, a wider announcement audience may be selected).

    Unlimited

13. ABSTRACT (a brief and factual summary of the document. It may also appear elsewhere in the body of the document itself. It is highly desirable that the abstract of classified documents be unclassified. Each paragraph of the abstract shall begin with an indication of the security classification of the information in the paragraph (unless the document itself is unclassified) represented as (S), (C), (R), or (U). It is not necessary to include here abstracts in both official languages unless the text is bilingual).

An Over-the-Horizon Radar (OTHR) has been deployed near Ottawa, Canada. Auroral echoes and ground echoes were analyzed in range, azimuth, elevation, and Doppler. It is shown that the auroral echoes and the ground echoes can be separated in elevation angle.

Un radar haute fréquence transhorizon à été déployé près d'Ottawa, Canada. Echos aurorales et échos de sol ont été analysées dans la gamme, l'azimut, l'élévation et Doppler. Il est démontré que les échos aurorales et les échos de sol peuvent être séparés dans l'angle d'élévation.

14. KEYWORDS, DESCRIPTORS or IDENTIFIERS (technically meaningful terms or short phrases that characterize a document and could be helpful in cataloguing the document. They should be selected so that no security classification is required. Identifiers, such as equipment model designation, trade name, military project code name, geographic location may also be included. If possible keywords should be selected from a published thesaurus. e.g. Thesaurus of Engineering and Scientific Terms (TEST) and that thesaurus-identified. If it not possible to select indexing terms which are Unclassified, the classification of each should be indicated as with the title).

radio
sky wave
high frequency
ionosphere
correlation
scintillation